

# Design of broadband RF pulses with polynomial-phase response

R.F. Schulte <sup>\*,1</sup>, A. Henning, J. Tsao <sup>2</sup>, P. Boesiger, K.P. Pruessmann

*Institute for Biomedical Engineering, University and ETH Zurich, Gloriastr. 35, 8092 Zurich, Switzerland*

Received 15 December 2006; revised 2 February 2007

Available online 4 February 2007

## Abstract

The achievable bandwidth of common linear-phase RF pulses is limited by the maximum feasible  $B_1$  amplitude of the MR system. It has been shown previously, that this limitation can be circumvented by overlaying a quadratic phase in the frequency domain, which spreads the power across the pulse duration. Quadratic-phase RF pulses are near optimal in terms of achieving minimal  $B_{1\max}$ . In this work, it is demonstrated that further  $B_{1\max}$  reduction can be achieved by combining quadratic with higher-order polynomial-phase functions. RF pulses with a phase response up to tenth order were designed using the Shinnar-Le Roux transformation, yielding considerable increases in bandwidth and selectivity as compared to pure quadratic-phase pulses. These benefits are studied for a range of pulse specifications and demonstrated experimentally. For  $B_{1\max} = 20 \mu\text{T}$  and a pulse duration of 2.1 ms, it was possible to increase the bandwidth from 3.1 kHz for linear and 3.8 kHz for a quadratic to 9.9 kHz for a polynomial-phase pulse.

© 2007 Elsevier Inc. All rights reserved.

**Keywords:** Polynomial-phase pulses; Shinnar-Le Roux transformation; Broadband RF pulses; Very selective saturation

## 1. Introduction

Shaped radio-frequency (RF) pulses are ubiquitous in all kinds of MR experiments. Their design is generally difficult due to the complex nature of the underlying spin dynamics. For MRI purposes, the latter are usually described by the Bloch equations, whose coupled differential equations are difficult to invert. One approach to the RF pulse design problem is the inverse scattering transformation (IST) [1–3]. The most widely used way to design RF pulses is the Shinnar-Le Roux (SLR) transformation [4], which reversibly converts an RF pulse into two finite impulse response (FIR) filters. The problem of inverting the Bloch equations is hence reduced to FIR filter design,

which is a highly advanced discipline in electrical engineering.

RF pulses have to fulfil several, often contradicting requirements. Besides high selectivity and short duration, a common desire is a large bandwidth for reducing artefacts such as chemical-shift displacement or curved slices. For regular linear-phase amplitude-modulated pulses, the bandwidth is tightly limited by the maximal allowed RF field strength ( $B_{1\max}$ ) of the transmitting. This limitation is related to the fact that linear-phase pulses concentrate the applied RF power in a central main lobe. The overall  $B_1$  of the pulse is scaled to this maximum in order not to exceed the system limitation although most of the time the necessary  $B_1$  is much lower. This represents an inefficient usage of available RF power. It is therefore desirable to design RF pulses with more efficient use of  $B_1$  amplitude and hence inherently broader bandwidths.

One way of achieving this is to overlay a quadratic phase onto the frequency response of the RF pulses, hence yielding frequency-modulated pulses. The central main lobe of the RF amplitude is spread out over a longer period of

\* Corresponding author.

E-mail address: [rolf.schulte@gmail.com](mailto:rolf.schulte@gmail.com) (R.F. Schulte).

<sup>1</sup> Present address: GE Global Research - Munich, Freisinger Landstr. 50, 85748 Garching, Germany.

<sup>2</sup> Present address: Novartis Institutes for BioMedical Research, Inc., Discovery Technologies, 250 Massachusetts Avenue, Cambridge MA 02139, USA.

the pulse, hence  $B_1$  efficiency of these pulses is increased. The disadvantage of non-linear phase pulses, however, is the inability of refocusing the phase by linear gradients. Therefore, these pulses cannot function as general excitation or refocusing pulses. Suitable applications are inversion or saturation of magnetisation, such as required for outer-volume suppression [5,6]. Non-linear-phase pulses can also be used for 3D imaging, where the pulse phase is resolved in through-slice direction [7]. Alternatively, the frequency modulation can also be used for actual image encoding [9,10].

It has been argued previously that pulses with an overlaid quadratic phase are near-optimal in terms of minimal  $B_{1\max}$  [5,11]. Ideal in terms of excitation profile and minimal  $B_{1\max}$  would be a rectangular envelope in both domains. A rectangular profile in the spectral domain represents a good excitation profile, and a rectangular profile in the temporal domain exhibits the most uniform distribution of power across the pulse duration, which is conserved according to Parseval's theorem. Mathematically, the near-optimality of the quadratic phase can be derived with an asymptotic series expansion [12]. The envelope (i.e., absolute value) of a function with an overlaid quadratic phase is the same in both time and frequency domain, assuming a smooth envelope and sufficient amount of quadratic phase [11,12]. For practical quadratic-phase pulses [5,11], both conditions are fulfilled to a large extent, but somewhat violated in detail. The first violation stems from the fact that a rectangular function contains discontinuities in the transition bands. The asymptotic series expansion can nevertheless be applied to the continuous areas of the function [12]. The second violation stems from the limit on the amount of quadratic phase applicable [11]. Therefore, quadratic-phase RF pulses are only near-optimal in terms of minimal  $B_{1\max}$ , suggesting that further reduction of  $B_{1\max}$  may be possible by deviating from a purely quadratic-phase response.

The objective of this work was hence to investigate how the quadratic-phase response can be modified in order to spread out the overall RF power even more effectively. To this end, the phase response is modelled generally as a polynomial of finite order. The effects of various monomial-phase responses are studied first. The minimal  $B_{1\max}$  is then approached by two different forms of non-linear optimisation, an exhaustive and a direct search. The exhaustive search is a systematic combination of quadratic with a single even-order phase, iterating through varying amounts of the two phase terms. The main benefit of an exhaustive search is to safely find the global optimum. However, it is highly time consuming, hence permitting only two parameters at a time to be optimised. The direct search algorithm allows more phase terms to be optimised at the same time, however there is no proof of reaching the global minimum. Using the direct search approach, pulses with a combination of 2nd–10th-order phases were designed for various parameter settings.

## 2. Methods

The SLR transformation reversibly transforms an RF pulse into two FIR filters, the “ $A$ ” and “ $B$ ” polynomials [4]. In this work, the  $B$  polynomial is designed with the complex Remez exchange algorithm [11,13,14], while the  $A$  polynomial is subsequently generated with the Hilbert transformation [4]. The complex Remez exchange algorithm fits a FIR filter polynomial to an arbitrary response function by minimising the Chebyshev (i.e., maximum) error norm, hence yielding equi-ripple error functions. The desired complex response function  $D$  is specified by

$$D(\omega) = R(\omega)e^{i\varphi(\omega)}, \quad (1)$$

where  $R(\omega)$  is the magnitude,  $\varphi(\omega)$  the phase response and  $\omega \in [-\pi, \pi]$  the normalised offset frequency [11]. In the scope of the present work, the phase function is modelled as

$$\varphi(\omega) = \sum_{\lambda \in A} k_\lambda \omega^\lambda, \quad (2)$$

where  $A$  is the set of polynomial phase orders considered and  $k_\lambda$  denotes the corresponding coefficients.

The target profile is a low-pass filter with its magnitude response specified by

$$R(\omega) = \begin{cases} 0 & \text{for } |\omega| \geq \omega_s \\ \sin\left(\frac{\theta}{2}\right) & \text{for } |\omega| \leq \omega_p \end{cases}, \quad (3)$$

where  $\theta$  is the desired flip angle. The pass and the stop band frequencies  $\omega_p$  and  $\omega_s$  are related to the bandwidth by

$$BW = \omega_s + \omega_p \quad (4)$$

and the fractional transition width by

$$FTW = \frac{\omega_s - \omega_p}{BW}. \quad (5)$$

The fitting error is related to these parameters by an empirical relationship [4] derived for equi-ripple FIR filters

$$D_\infty = n \cdot BW \cdot FTW = f(\delta_1, \delta_2), \quad (6)$$

where  $n$  is the number of samples (i.e., normalised time [11]).  $D_\infty$  is also a function of the error amplitudes  $\delta_1$  and  $\delta_2$  in the pass and stop bands, respectively [4]. This relationship was derived for linear-phase filters. For the present study it was hypothesised that it holds approximately for polynomial-phase pulses as well. Hence, Eq. (6) was used throughout to calculate  $n \cdot BW \cdot FTW$  from given error specifications. The validity of this approach was then verified by checking the actual resulting ripple amplitudes.

In the following and as introduced in Ref. [11], the tilde symbol denotes physical units, which are related to the normalised units from FIR filter design by

$$\tilde{T} = n\Delta\tilde{t}, \quad (7)$$

where  $\tilde{T}$  denotes the pulse duration and  $\Delta\tilde{t}$  the sample spacing. The number of samples  $n$  is equivalent to the normalised time. The physical RF amplitude is given by

$$\tilde{B}_1 = \frac{B_1}{\gamma \Delta t}, \quad (8)$$

and the bandwidth by

$$\tilde{B}\tilde{W} = \frac{B\tilde{W}}{\Delta t}, \quad (9)$$

leading to the time-bandwidth product

$$\tilde{T} \cdot \tilde{B}\tilde{W} = n \cdot B\tilde{W}. \quad (10)$$

The achievable bandwidth of RF pulses can be increased by minimising the  $B_{1\max}$  of the pulse. The underlying relationship between  $B_{1\max}$  and the physical bandwidth  $\tilde{B}\tilde{W}$  can be derived by equating  $\Delta t$  in Eqs. (8) and (9) and multiplying both sides with  $n$

$$nB_{1\max} = \tilde{B}_{1\max} \gamma \frac{n \cdot B\tilde{W}}{\tilde{B}\tilde{W}}. \quad (11)$$

With a fixed physical  $\tilde{B}_{1\max}$  of the system, gyro-magnetic ratio  $\gamma$  and time-bandwidth product  $n \cdot B\tilde{W}$ , Eq. (11) translates into the following anti-proportionality

$$\tilde{B}\tilde{W} \propto \frac{1}{nB_{1\max}}, \quad (12)$$

where  $B_{1\max}$  is the maximum pulse amplitude in normalised units. Hence, the key dependence of bandwidth limits on the feasible  $B_{1\max}$  is confirmed.

The optimisation problem is to find the phase polynomial yielding the minimal  $B_{1\max}$  for a given set of parameters. An RF pulse is typically specified by the flip angle  $\theta$ , the time-bandwidth product  $n \cdot B\tilde{W}$  and the fractional transition width FTW. Side-constraints are an acceptable error  $\delta$  ( $=\delta_1 = \delta_2$ ) of the response function and a sufficient number of samples  $n$  in order to fulfil the hard-pulse approximation inherent to the SLR approach [4].

The first step in exploring the phase polynomial was to design RF pulses with monomial phases of up to tenth order and investigate their  $B_{1\max}$  behaviour. Subsequently, the minimal  $B_{1\max}$  was approached by an exhaustive search. This kind of optimisation generally finds the global optimum, however it is computationally demanding permitting in our case only two phase terms to be optimised simultaneously. Therefore, a quadratic phase was systematically combined with one other higher even-order phase up to ten at a time (i.e.,  $A = \{2,4\}$ ;  $A = \{2,6\}$ ;  $A = \{2,8\}$ ;  $A = \{2,10\}$ ). The minimum- $B_{1\max}$  solution with an acceptable error was identified within the resulting two-dimensional parameter landscape.

Finally, a direct search method was implemented for finding the optimal combination of more than two phase terms. Direct search algorithms are preferable to gradient-descent methods, because the cost function is not sufficiently smooth and its gradients cannot be calculated analytically. The cost function for the direct search minimisation was chosen as

$$\kappa = B_{1\max}^2 + P_\delta^2, \quad (13)$$

where  $P_\delta$  is a penalty term given by

$$P_\delta = \begin{cases} 0 & \text{for } \delta < \delta_0 \\ \eta(\delta - \delta_0) & \text{for } \delta \geq \delta_0 \end{cases}, \quad (14)$$

with  $\delta$  ( $=\delta_1 = \delta_2$ ) being the equi-ripple error of the FIR filter response,  $\delta_0$  the maximum tolerable error and  $\eta$  a scaling factor for controlling convergence. The direct search is repeated three times with each successive optimisation being initialised by the previous one. The first two stages use a pattern-search algorithm [15], initialised with the amount of quadratic phase from the empirical limit (Eq. 19 in [11]) and zero for all other phase terms. The last optimisation stage applies a Nelder–Mead Simplex algorithm [15]. The penalty factor  $\eta$  was increased during the three stages (for  $n = 256$ ,  $\eta$  was 0.05, 1, and 100).

All numerical procedures were implemented in MATLAB V7.0 SP2 (R14) (The MathWorks, Natick, MA, USA). The pattern search algorithm uses the MATLAB function “patternsearch” in the “Genetic Algorithm and Direct Search Toolbox”, while the Nelder–Mead Simplex method applies the function “fminsearch” from the “Optimisation Toolbox”. The complex Remez exchange algorithm uses the function “cfirpm” (formerly “cremez”) from the “Signal Processing Toolbox”. MRI experiments were performed on a Philips Achieva 3 T scanner equipped with a transmit/receive head coil allowing for a  $\tilde{B}_{1\max} = 20 \mu\text{T}$  (Philips Medical Systems, Best, The Netherlands).

### 3. Results and discussion

RF pulses with monomial phase functions are depicted in Fig. 1. Odd-order phase functions (left) lead to purely amplitude-modulated pulses, while even orders result in frequency-modulated pulses. A third-order phase ( $A = \{3\}$ ) leads to an asymmetric pulse shape. Hence,  $B_{1\max}$  is reduced by distorting the central main lobe to give about equal positive and negative heights (Fig. 1) according to empirical findings. The possible reduction, however, is not more than roughly half the original height. It was observed, that the  $B_{1\max}$  reduction achievable with odd-order phases is limited by the fact that the energy of the RF main-lobe is mainly distributed towards one side only. Thus, it should be possible to further reduce  $B_{1\max}$  by spreading the central main lobe symmetrically, which can be achieved with even-order phases (Fig. 1, right side). The area of spreading out  $B_1$  is increasingly contained to the central part of the RF pulse with an increased order. Of all the monomial-phase functions, the quadratic phase spreads the central main lobe over the widest area of the pulse, hence supporting the  $B_{1\max}$  near-optimality argument [11]. Only a combination of quadratic with higher even-order phase functions ( $A = \{2,4,6,8,10\}$ ) distributes the energy even further.

The  $B_{1\max}$  for a systematic combination of quadratic with a single higher even-order phase (i.e.,  $A = \{2,4\}$ ,  $A = \{2,6\}$ ,  $A = \{2,8\}$ ,  $A = \{2,10\}$ ) is shown in Fig. 2 for pulses with the same target profile. With each combination

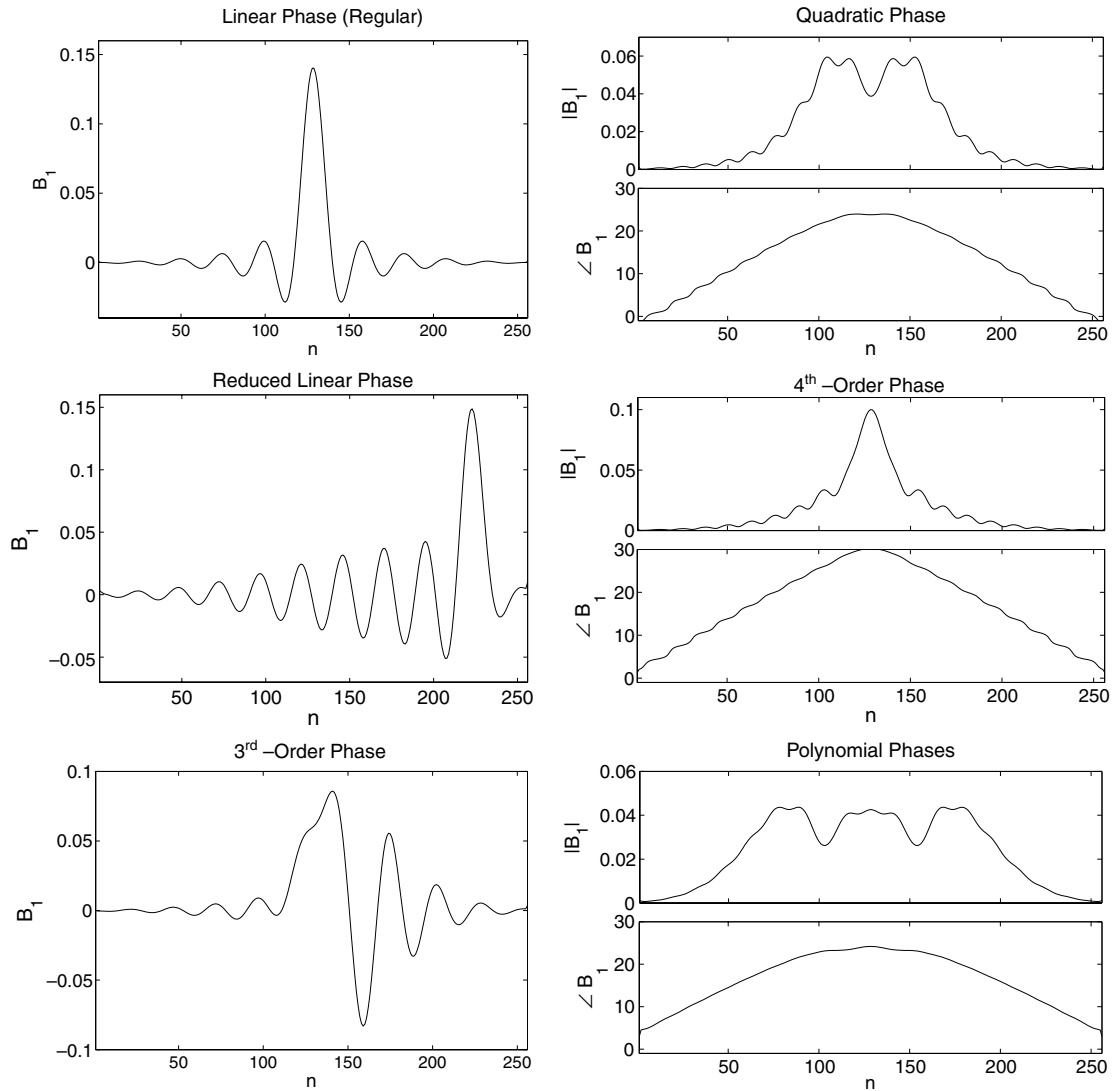


Fig. 1. Various kinds of pulses all designed with different phase functions but the same target profile ( $\theta = 90^\circ$ ;  $n \cdot \text{BW} = 130$ ,  $D_\infty = 20$ ; which leads with  $n = 256$  to  $\text{BW} = 0.508$  and  $\text{FTW} = 0.154$ ). The high time-bandwidth product of 130 (in radians) leads to a fairly large amount of side-lobes. On the left side are RF pulses with single odd-order-phase functions, which lead to pure amplitude modulation. The (partially) self-refocused linear-phase pulse leaves a reduced phase at the end of the excitation period, which corresponds to moving the temporal reference point further to the end of the RF pulse. Adding even-order-phase functions (right side) yield complex FIR filter coefficients and hence phase-modulated pulses. The polynomial-phase pulse combines even orders up to ten ( $A = \{2, 4, 6, 8, 10\}$ ).

it is possible to further reduce  $B_{1\text{max}}$  as compared to a pure quadratic phase (Table 1). The design parameters for these polynomial-phase pulses seem to be subject to certain restrictions, similar to pure quadratic-phase pulse design [11]. In particular, this means that not all parameter specifications result in acceptable pulses with a low fitting error. In this example the error limit was set to  $\delta < 0.00125$ . Under this constraint, the minimal  $B_{1\text{max}}$  was found for a combination of 2nd and 8th order ( $k_2 = 226$ ,  $k_8 = -186 \cdot 10^3$ ) (Table 1).

A further reduction of  $B_{1\text{max}}$  is possible by optimising a combination of more higher-order polynomial-phase terms with the direct search method (Table 1). Various polynomial schemes ( $A$ ) were considered in order to investigate the underlying relations. Higher even-order phase terms

( $A = \{2, 4, 6, 8, 10\}$ ) were compared to all higher-order phase terms up to ten ( $A = \{1, 2, 3, \dots, 10\}$ ) in order to further support the argument that odd orders are not useful for reducing  $B_{1\text{max}}$ . Although the optimisation indeed yielded contributions of odd orders as well, the resulting  $B_{1\text{max}}$  was larger with odd orders included. Therefore, only combinations of even-order phase terms are considered in the following investigations.

The influence of the selection of the various phase terms on the RF pulses were investigated by optimising polynomial-phase functions ( $A = \{2, 4, 6, 8, 10\}$ ) with various fitting errors ( $\delta = 0.032$ , 0.0056, 0.00125 and 0.00032), reflected by empirical performance measures of  $D_\infty = 10$ , 15, 20 and 25, respectively. Time-bandwidth products  $n \cdot \text{BW}$  ranged from 30–500 in steps of 5 (in radians), result-

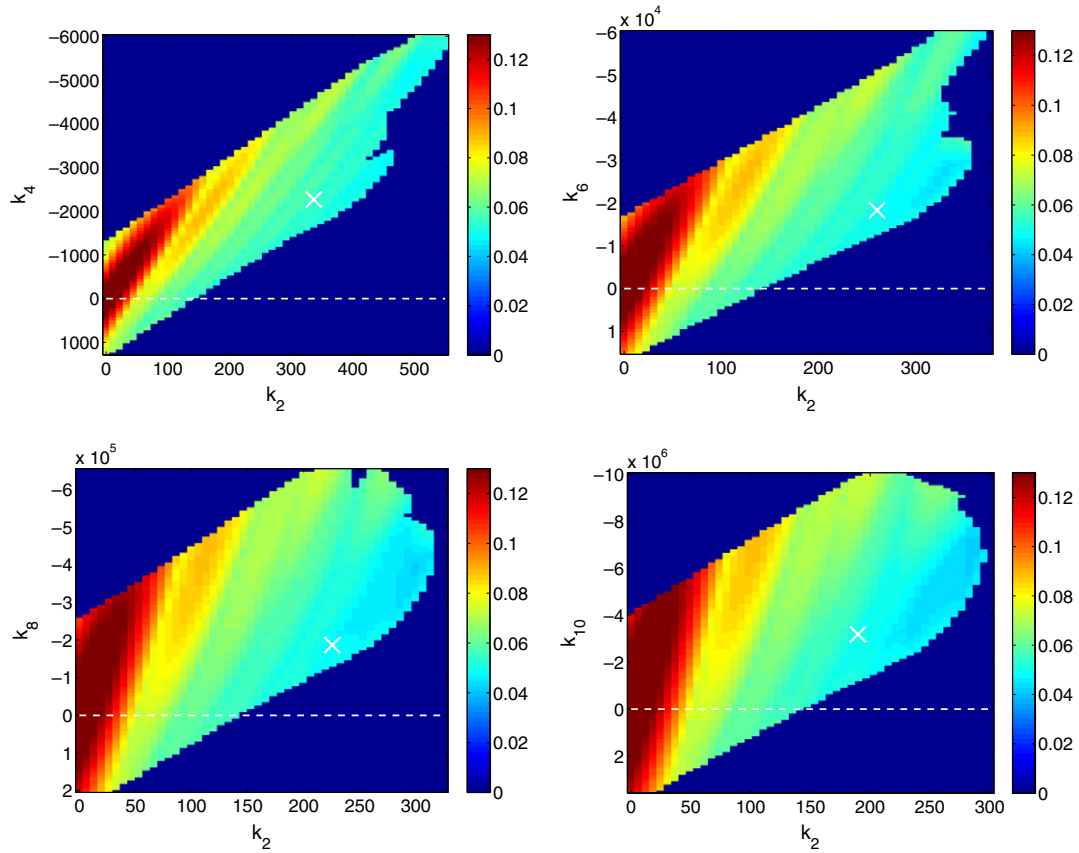


Fig. 2. Maps of  $B_{1\max}$  (colour scale) for different amounts of 2nd ( $k_2$ ; x-axis) and higher (4th, 6th, 8th, and 10th) order phase ( $k_i$ ; y-axis) for pulses with the same target profile as in Fig. 1. The dashed white line exhibits pure quadratic phase. Due to symmetry, only positive  $k_2$  are shown. The blue outer region with excessive fitting errors ( $\delta > 0.05$ ) is excluded because of meaningless results. The minimal  $B_{1\max}$  with an acceptable error ( $\delta \leq 0.00125$ ) is marked with a white cross for each combination and listed in Table 1. Note that the  $x$  ( $k_2$ ) and  $y$  ( $k_i$ ) axes have different scales. (For interpretation of the references to colour in this figure legend, the reader is referred to the web version of this paper.)

Table 1

Different reductions of  $B_{1\max}$  relative to the linear-phase design ( $n \cdot \text{BW} = 130$ ,  $D_\infty = 20$ ; same as in Figs. 1 and 2)

Optimisation	Phase	$B_{1\max}$	Rel. to linear (%)	$\tilde{T}$ [ms]	$\tilde{\text{BW}}$ [kHz]
No	Linear	0.1402	100	6.7	3.1
Empirical [11]	2nd	0.0594	42.4	2.8	7.3
Exhaustive	2nd + 4th	0.0527	37.6	2.5	8.2
	2nd + 6th	0.0485	34.6	2.3	8.9
	2nd + 8th	0.0468	33.4	2.2	9.2
	2nd + 10th	0.0484	34.5	2.3	8.9
Direct	Combination	0.0436	31.1	2.1	9.9

$B_{1\max}$  is given in normalised units (Eq. 8). The physical time  $\tilde{T}$  and bandwidth  $\tilde{\text{BW}}$  are for a maximal RF field strength of  $\tilde{B}_{1\max} = 20 \mu\text{T}$ . The best combination found with the exhaustive search method for pairs of phase orders is  $\mathcal{A} = \{2, 8\}$ . This minimum can be further reduced with the direct search method when using a polynomial combination of phases ( $\mathcal{A} = \{2, 4, 6, 8, 10\}$ ).

ing in fractional-transition widths according to  $\text{FTW} = D_\infty / (n \cdot \text{BW})$  (Eq. (6)). The resulting RF pulses are then scaled to  $\tilde{B}_{1\max} = 20 \mu\text{T}$ , hence resulting in different pulse durations  $\tilde{T}$  and physical bandwidths  $\tilde{\text{BW}}$ . The relationship between  $\tilde{T}$  and  $\tilde{\text{BW}}$  for polynomial as well as for quadratic and linear-phase pulses with the same parameter specifications is depicted in Fig. 3. The optimisation scheme did not always converge, yet it found several suitable minima for a range of time-bandwidth products. As Fig. 3 suggests, the successfully optimised

pulses are grouped approximately along a straight line, reflecting a linear increase in bandwidth as a function of the pulse duration. To indicate this heuristic relationship, the favourable pulses are marked by circles and fitted by linear regression. Each pulse was considered favourable if it achieved a higher bandwidth than any previous pulse with a lower time-bandwidth product. These results show a considerably increased bandwidth for the polynomial-phase functions. This advantage is especially pronounced for pulses with low fitting errors

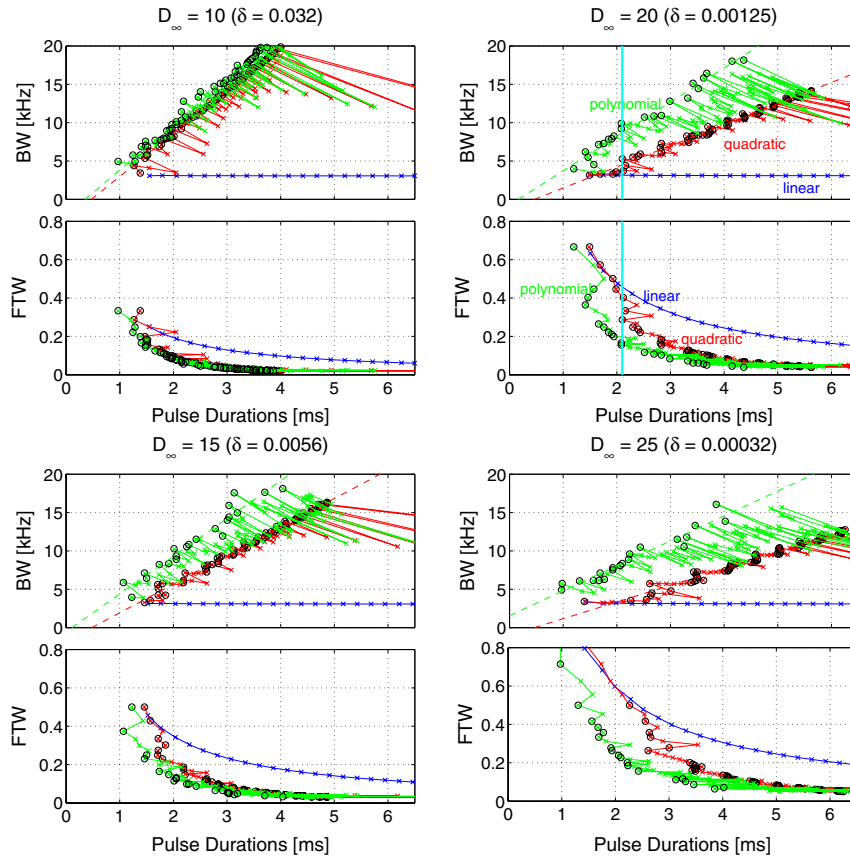


Fig. 3. The physical bandwidth  $\tilde{B}W$  and the fractional-transition width FTW plotted against the actual pulse durations for  $\tilde{B}_{1\max} = 20 \mu\text{T}$ . The time-bandwidth products increase from left (30) to right (500) in steps of 5. All points with an increase in bandwidth from one time-bandwidth product to the other are marked by circles and fitted by a linear regression curve. All other points with the wiggles pointing right, are sub-optimal parameter combinations or poor fits and should be discarded. Interesting to note in the plots is that the polynomial phase is especially advantageous for pulses with a high performance factor  $D_\infty$  and hence low errors. Three pulses (linear, quadratic and polynomial) with  $D_\infty = 20$  (top right, line in magenta) were selected and compared in Fig. 5. (For interpretation of the references to colour in this figure legend, the reader is referred to the web version of this paper.)

(i.e., high  $D_\infty$ ), while at  $D_\infty = 10$  the regression lines of quadratic and polynomial phase are approximately the same. The error in the FIR filter response is generally not considerably increased, as indicated in Fig. 4. This supports the assumption made in Eq. (6), that the empirically derived performance measure  $D_\infty$  is also valid for polynomial-phase pulses.

Linear-phase pulses (blue in Fig. 3) exhibit always the same bandwidth, while the selectivity improves with a higher time-bandwidth product (decreasing FTW in Eq. (6)). Both quadratic (red in Fig. 3) and polynomial (green in Fig. 3) phase pulses lead to an approximately linear increase in bandwidth as a function of pulse duration along with further enhanced selectivity. Polynomial-phase functions have basically two advantages over quadratic ones: the gain in bandwidth starts earlier and the slope of the regression line is steeper throughout. The gain in bandwidth is especially considerable for shorter pulse durations, which is crucial for good outer-volume suppression. Broad bandwidth comes along with high selectivity, which is therefore also better for polynomial-phase pulses. Again, this advantage is particularly pronounced for short pulse durations.

Interesting to note is the nature of the polynomial-phase modulation. While the quadratic-phase term is increased, the higher-order term attenuates the phase modulation close to the transition bands. The qualitative behaviour is visible in the  $B_{1\max}$  maps (Fig. 2) as well as in the excitation profile (Fig. 5). The attenuation is contained mainly near the transition bands, where the optimality argument of Papoulis [12] for quadratic phase is violated.

One of the main applications of polynomial-phase pulses is outer-volume suppression. Important for a successful saturation of magnetisation are short pulses with a broad bandwidth, high selectivity and low errors in the remaining magnetisation. A whole range of linear, quadratic and polynomial-phase pulses, all with  $D_\infty = 20$ , was designed and implemented into the scanner software for outer-volume suppression. The parameters of the selected polynomial-phase pulses are listed in Table 2. Pulses with a maximum duration of 3 and 5 ms were selected and their suppression profiles were measured in a water-oil phantom and in the human brain (Fig. 6). The chemical-shift displacement artefact is considerably reduced, while the selectivity is enhanced for pulses with a polynomial-phase response, as compared to both linear and quadratic phase.

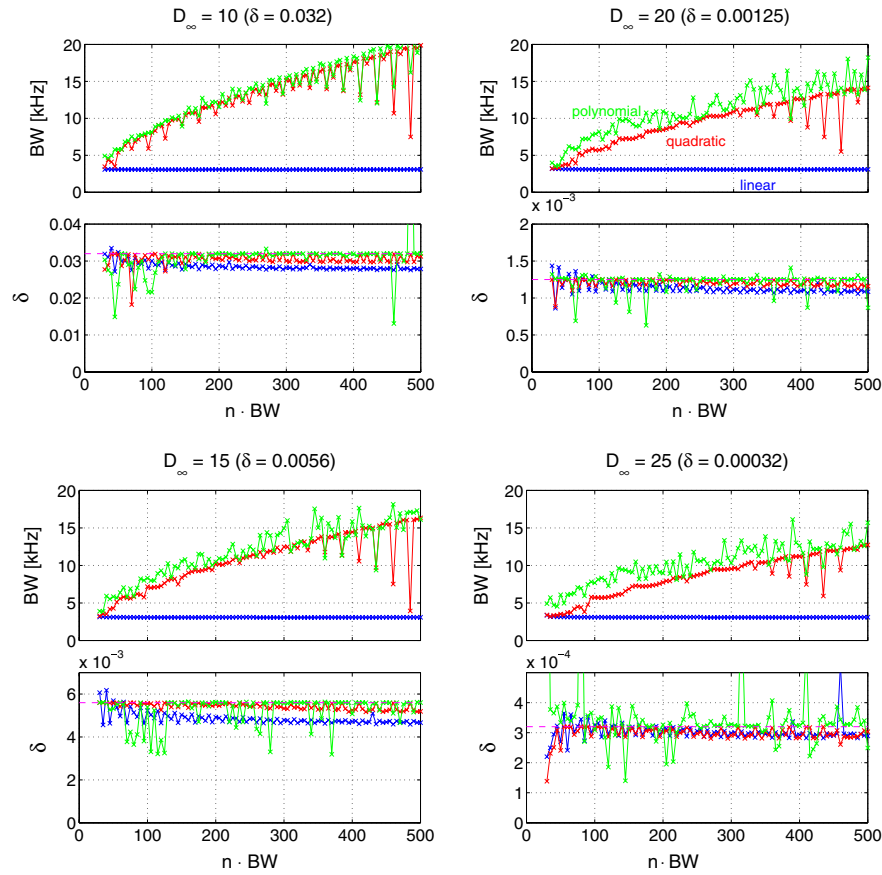


Fig. 4. The physical bandwidth  $\tilde{B}W$  and the error of the FIR filter response plotted against the time-bandwidth product  $n \cdot BW$ . This plot illustrates, that the proposed fitting procedure does not lead to a significantly increased error. However, the errors of non-linear phase pulses are slightly increased. In order to compensate for this effect and provide an equitable comparison, slightly smaller  $D_\infty$  were used for linear-phase pulses (7.5, 13.7, 19, and 23.9; instead of 10, 15, 20, and 25, respectively).

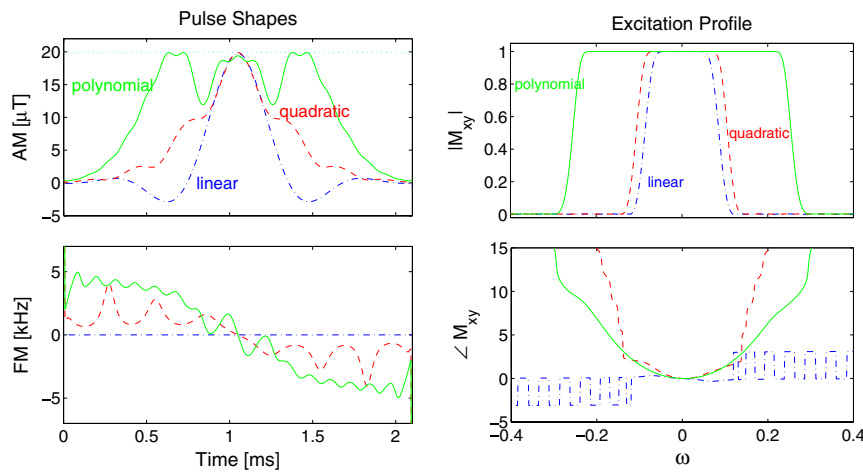


Fig. 5. RF pulses with the same  $\tilde{B}_{1\max}$  (20  $\mu\text{T}$ ) and duration ( $\tilde{T} = 2.1$  ms), but various phase functions. The bandwidth is increased from 3.1 kHz for a linear and 3.8 kHz for a quadratic to 9.9 kHz for a polynomial-phase pulse.

#### 4. Conclusions and outlook

Polynomial-phase pulses achieve both very broad bandwidths and high selectivities. They are particularly beneficial for short pulse durations and high performance  $D_\infty$  (i.e., low errors and small transition widths). For a typical

$\tilde{B}_{1\max} = 20 \mu\text{T}$  (whole-body 3 T scanner) and pulse duration of 2 ms, the bandwidth was increased from 3 kHz (linear-phase) to 10 kHz (polynomial-phase pulse). The advantages seem to be related to the fact that the phase variation is attenuated in the transition bands by the more local, higher-order polynomial-phase terms.

Table 2  
Pulse parameters for various favourable pulses selected from Fig. 3 for  $D_\infty = 20$  and  $n = 256$

$n \cdot \text{BW}$	$B_{1\text{max}}$	$k'_2$	$k'_4$	$k'_6$	$k'_8$	$k'_{10}$
30	0.0251	33.485	-26.498	-20.247	-24.582	-26.925
55	0.0295	21.097	-4.489	-11.472	3.048	-10.353
75	0.0347	17.652	6.354	4.153	-8.027	-6.029
100	0.0406	15.775	5.773	-5.808	-4.647	-5.506
130	0.0436	11.845	5.452	-2.440	-3.276	-4.541
170	0.0526	10.416	4.340	-2.251	-0.307	-3.454
240	0.0624	8.529	3.522	-1.435	1.130	-2.500

Note that both  $B_{1\text{max}}$  and  $k'_\lambda$  depend on  $n$ . The amount of phase is given by  $k_\lambda = \text{sign}(k'_\lambda)|k'_\lambda|^\lambda$ .

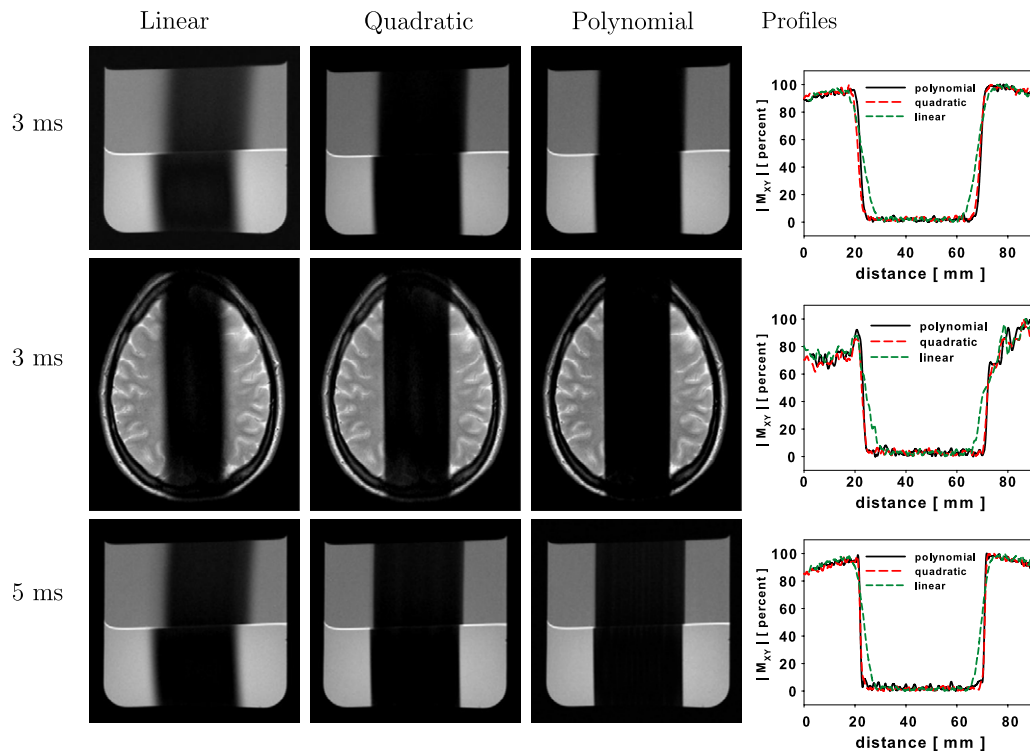


Fig. 6. Various suppression profiles for maximum pulse durations of 3 and 5 ms. Profiles are measured in a water–oil phantom and in the human brain. The gradient strength was scaled to the according bandwidth in order to excite always the same slice thickness. Due to the higher bandwidth and gradient strength, the chemical-shift displacement can be considerably reduced. Note, that the  $B_1$  inhomogeneities commonly present on 3 T scanners lead to a degradation of profiles, here especially pronounced in the oil section for the linear-phase pulse. The right hand side shows the cross-section through the water section in the lower part of the phantom.

Polynomial-phase pulses have great potential for outer-volume suppression, particularly for whole-body scanners with higher field strengths. Outer-volume suppression is generally most effective when the time between the suppression pulses and the acquisition is short. This places tight constraints on both RF pulse durations and gradient times. Polynomial-phase pulses are particularly beneficial for short pulse durations, hence they can considerably enhance outer-volume suppression.

#### Acknowledgment

The authors thank Philips Medical Systems for technical and financial support.

#### References

- [1] A.E. Yagle, Inversion of the Bloch transformation in magnetic resonance imaging using asymmetric two-component inverse scattering, *Inverse Problems* 6 (1990) 133–151.
- [2] C.L. Epstein, Minimum energy pulse synthesis via the inverse scattering transform, *J. Magn. Reson.* 167 (2004) 185–210.
- [3] J. Magland, C.L. Epstein, Practical pulse synthesis via the discrete inverse scattering transform, *J. Magn. Reson.* 172 (2005) 63–78.
- [4] J.M. Pauly, P. Le Roux, D.G. Nishimura, A. Macovski, Parameter relations for the Shinnar-Le Roux selective excitation pulse design algorithm, *IEEE T Med. Imaging* 10 (1) (1991) 53–65.
- [5] P. Le Roux, R.J. Gilles, G.C. McKinnon, P.G. Carrier, Optimized outer volume suppression for single-shot fast spin-

- echo cardiac imaging, *J. Magn. Reson. Imaging* 8 (5) (1998) 1022–1032.
- [6] T.K.C. Tran, D.B. Vigneron, N. Sailasuta, J. Tropp, P. Le Roux, J. Kurhanewicz, S. Nelson, R. Hurd, Very selective suppression pulses for clinical MRSI studies of brain and prostate cancer, *Magn. Reson. Med.* 43 (1) (2000) 23–33.
- [7] J.Y. Park, L. DelaBarre, M. Garwood, Improved gradient-echo 3D magnetic resonance imaging using pseudo-echoes created by frequency-swept pulses, *Magn. Reson. Med.* 55 (4) (2006) 848–857.
- [9] Y. Shrot, L. Frydman, Spatially encoded NMR and the acquisition of 2D magnetic resonance images within a single scan, *J. Magn. Reson.* 172 (2) (2005) 179–190.
- [10] A. Tal, L. Frydman, Spatial encoding and the single-scan acquisition of high definition MR images in inhomogeneous fields, *J. Magn. Reson.* 182 (2) (2006) 179–194.
- [11] R.F. Schulte, J. Tsao, P. Boesiger, K.P. Pruessmann, Equi-ripple design of quadratic-phase RF pulses, *J. Magn. Reson.* 166 (1) (2004) 111–122.
- [12] A. Papoulis, *Signal Analysis*, McGraw-Hill, New York, 1977, Ch. 8, ISBN 0-07-048460-0.
- [13] L.J. Karam, J.H. McClellan, Complex Chebyshev approximation for FIR filter design, *IEEE T Circuits-II* 42 (3) (1995) 207–216.
- [14] L.J. Karam, J.H. McClellan, Chebyshev digital FIR filter design, *Signal Process.* 76 (1) (1999) 17–36.
- [15] MATLAB Documentation, The MathWorks, Natick, MA, USA, <http://www.mathworks.com/access/helpdesk/help/helpdesk.html>.